The Cryosphere, 8, 1445–1456, 2014
www.the-cryosphere.net/8/1445/2014/
doi:10.5194/tc-8-1445-2014
© Author(s) 2014. CC Attribution 3.0 License.

The Cryosphere Open Access

Recent ice dynamic and surface mass balance of Union Glacier in the West Antarctic Ice Sheet

A. Rivera[1,2], R. Zamora[1], J. A. Uribe[1], R. Jaña[3], and J. Oberreuter[1]

[1]Centro de Estudios Científicos, P.O. Box 5110466, Valdivia, Chile
[2]Departamento de Geografía, Universidad de Chile, P.O. Box 3387, Santiago, Chile
[3]Instituto Antártico Chileno, Punta Arenas, Chile

Correspondence to: A. Rivera (arivera@cecs.cl)

Received: 31 December 2013 – Published in The Cryosphere Discuss.: 20 February 2014
Revised: 22 May 2014 – Accepted: 15 June 2014 – Published: 6 August 2014

Abstract. Here we present the results of a comprehensive glaciological investigation of Union Glacier (79°46′ S/83°24′ W) in the West Antarctic Ice Sheet (WAIS), a major outlet glacier within the Ellsworth Mountains. Union Glacier flows into the Ronne Ice Shelf, where recent models have indicated the potential for significant grounding line zone (GLZ) migrations in response to changing climate and ocean conditions. To elaborate a glaciological base line that can help to evaluate the potential impact of this GLZ change scenario, we installed an array of stakes on Union Glacier in 2007. The stake network has been surveyed repeatedly for elevation, velocity, and net surface mass balance. The region of the stake measurements is in near-equilibrium, and ice speeds are 10 to 33 m a^{-1}. Ground-penetrating radars (GPR) have been used to map the subglacial topography, internal structure, and crevasse frequency and depth along surveyed tracks in the stake site area. The bedrock in this area has a minimum elevation of −858 m a.s.l., significantly deeper than shown by BEDMAP2 data. However, between this deeper area and the local GLZ, there is a threshold where the subglacial topography shows a maximum altitude of 190 m. This subglacial condition implies that an upstream migration of the GLZ will not have strong effects on Union Glacier until it passes beyond this shallow ice pinning point.

1 Introduction

WAIS, the West Antarctic Ice Sheet (Fig. 1), has been considered potentially unstable because its bedrock is located well below sea level (Bamber et al., 2009) and its total disintegration could contribute up to 4.3 m (Fretwell et al., 2013) to global sea-level rise. In many cases, the topography underneath WAIS is inversed (ice is deeper upstream) and steeper than in the present grounding line zones (GLZ) (Ross et al., 2012). This topographic condition, in the context of ongoing global changes, especially oceanic warming in areas of the Southern Ocean, is leading to GLZ upstream migration, as observed for example in the Amundsen Sea Embayment area (ASEA) glaciers like Pine Island (PIG) and Thwaites (Rignot et al., 2002). This migration process in the context of inversed subglacial topographies has an impact on glacier dynamics, since bottom melting at the GLZ is higher in deeper waters, provoking higher ice fluxes, ice thinning and, in general, a more negative mass balance (Rignot and Jacobs, 2002). However, there are WAIS areas where the changes are not as dramatic as observed in ASEA, with some regions thickening rather than thinning (Joughin and Bamber, 2005).

One of the WAIS areas where glaciological changes are not strong at present is the Weddell Sea sector (Rignot and Thomas, 2002), where the Ronne Ice Shelf (RnIS) is located (Fig. 1). This floating platform has been relatively stable in recent decades, with different behaviours of the GLZ and very small net mass balance changes (Rignot et al., 2011b). The relative stability of the RnIS is partly explained by the Weddell Seas oceanographic and atmospheric conditions, and the associated broad extent of sea ice (Mayewski et al., 2009). The sea ice extent in this area has been stable (Cavalieri and Parkinson, 2008), but recent studies (Hellmer et al., 2012) forecast a sea ice volume reduction for the twenty-first century, resulting in incremental circulation of warm water beneath the Filchner Ice Shelf toward the GLZ of the Slessor, Recovery, Support Force, Möller and Foundation ice streams. The intrusion of warmer waters will certainly increase the basal melt rate of the ice shelf, and possibly lead

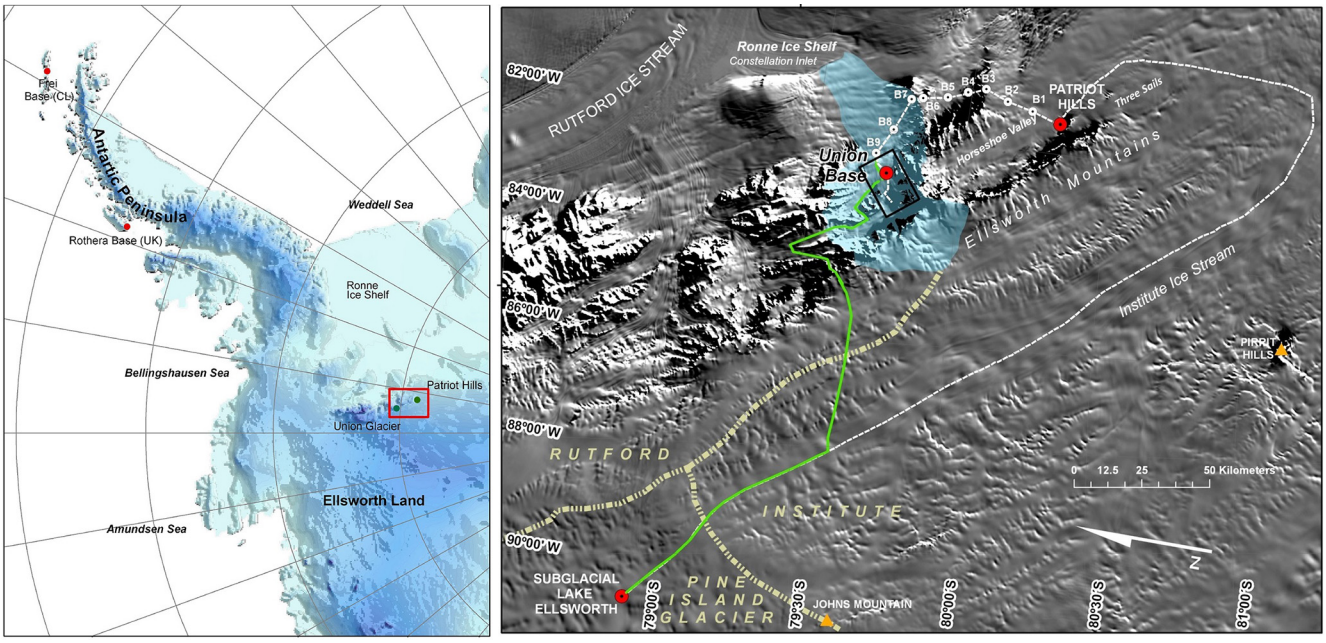

Figure 1. Left: WAIS location map. Right: Union Glacier basin (light-blue area). In yellow, the main ice divides in the region. In dashed white the 2005 track to subglacial Lake Ellsworth (517 km). In green, the new track surveyed in 2010 (235 km). Stakes B1 to B9 are described in the text. The black box is shown in Fig. 2. Background image: MODIS Mosaic of Antarctica (MOA: Scambos et al., 2007).

to retreat of the GLZ. This, in turn, would favour higher ice fluxes along tributary glaciers, and thinning that will spread upstream along deep channels (Rignot et al., 2011b).

Between two of the main ice streams in the region (Rutford and Institute), there are two smaller glaciers also draining into the RnIS: Union Glacier (79°46′ S/83°24′ W) flowing into Constellation Inlet, and the Horseshoe Valley glacier (80°18′ S/81°22′ W) flowing into Hercules Inlet. The study of these glaciers could provide an important clue about ongoing changes taking place in the region, especially considering that local glacier mass balance can be significantly affected by RnIS changes.

In this context, the main aim of this paper is to present recent glaciological results obtained at Union Glacier and nearby areas that provide a base line for possible ice dynamic responses to ongoing and modelled future changes of RnIS.

2 Study area

Union Glacier (79°46′ S/83°24′ W) (Fig. 2) has an estimated total area of 2561 km^2, with a total length of 86 km from the ice divide with the Institute Ice Stream down to the grounding line of Constellation Inlet on the RnIS. The glacier has several glacier tributaries, the main trunks being located in the Union and Schanz valleys (Figs. 1 and 2), which are fed through narrow glacial valleys (9 km wide) flowing from the interior plateau until they merge at the Union "gate". This gate or narrowest section of the glacier (7 km wide) has a medial moraine line comprised of clasts and small-sized debris.

The local Union Glacier blue ice area (BIA) is used for landing Ilyushin IL76 airplanes on wheels under a contract with the private company Antarctic Logistics and Expeditions (ALE) llc. This company has been operating in the region since the 1980s, when they began to use the Patriot Hills BIA (Wendt et al., 2009) at Horseshoe Valley (80°18′ S/81°22′ W) for landing heavy airplanes. However, these airplane operations were frequently disrupted due to strong prevailing cross winds at Patriot Hills. In order to increase the number of airplane operational days and to improve access for heavy cargo airplanes, in 2007/8 ALE moved to Union Glacier, where the prevailing wind direction is in line with the landing strip (katabatic winds), helping airplanes to operate even with strong gusts. Thanks to ALE logistic support, four scientific campaigns have been conducted on Union Glacier since 2008, where a glaciological program was established, including ice dynamics, mass balance and geophysical surveys (Rivera et al., 2010).

An array of 21 stakes was installed at the gate in 2007 for ice dynamic and surface mass balance studies. The Union gate has been re-surveyed by using GPS and radar systems installed onboard convoys pulled by Camoplast tractors travelling along pre-designated routes. Results of the first campaigns of 2007 and 2008 were published by Rivera et al. (2010).

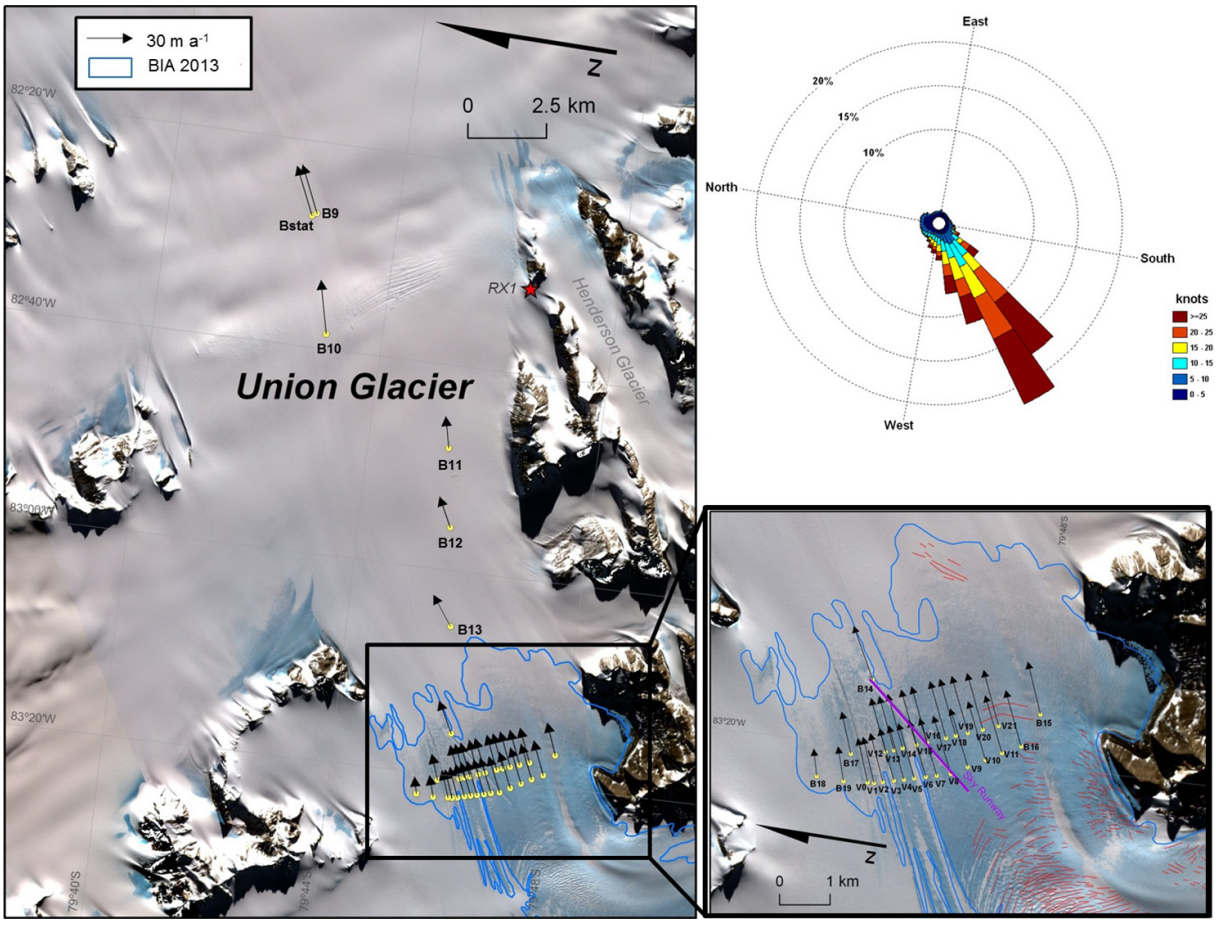

Figure 2. Yellow dots show the stakes described in the text (Fig. 1 and Table 2). RX1 is the location of the static GPS on rock. Crevasses are shown in red. The Union Glacier "gate" is a transversal profile between B18 and B15 (inset) where the ice runway is shown in purple. Mean ice velocity area shown as arrows. Summer base camp is visible near B11. The background image is an ASTER false composite 321 acquired on 1 February 2013. Upper right: predominant wind speed and direction for 2008–2012 at the Union Glacier automatic weather station, installed near stake V17.

3 Methods

3.1 Meteorological data

The meteorological data analysed here were collected at the Union Glacier automatic weather station (AWS) installed near stake V17, which has been operating since 2008 (Fig. 2). The AWS data series show several data gaps due to malfunction or low power supply problems during the winter. In spite of these, the available data are good enough for weather forecasts during landing operations in the summer, and for describing general temperature conditions in the area as well as predominant winds and directions.

3.2 Remote sensing

Mid-summer ASTER satellite images acquired between 2002 and 2013 (Table 1) were analysed and classified via manual digitalisation in order to delineate the local Union Glacier main BIA. This task allowed areal changes in snow cover to be quantified and analysed for possible relationships with local meteorological data.

Table 1. BIA extension based upon ASTER images collected since 2002.

Year/month/day	Area (km^2)
2002/11/24	95.6
2004/12/09	104.7
2007/01/27	112.0
2009/01/17	111.8
2012/02/11	88.2
2013/02/01	96.7

The ASTER images were corrected geometrically using the internal parameters of each scene. A true colour composition (bands 1, 2 and 3N) for each year was produced and

the contrast and brightness modified by means of histogram equalisation to facilitate the delimitation of the blue ice area.

The BIA outline mapping was based upon a similar procedure established by Rivera et al. (2014), where the boundary between snow and ice is identified manually assuming the maximum extent criterion of identification. This is easily done thanks to the spectral differences between snow and ice.

3.3 Glaciological mass balance

Stake heights above the snow/ice surface were measured yearly between 2007 and 2011 (Figs. 1 and 2; Table 2). Of 88 potential stake measurements at the gate, 72 were acquired successfully. The annual heights were compared and local mass balance was subsequently calculated. In order to convert these values into their water equivalent, a mean density of 910 kg m^{-3} (Paterson, 1994) was used for stakes drilled on ice. In those cases where the stakes were located at snow surfaces, the densities were measured by using a Mount Rose snow probe with a penetration capacity of near 50 cm of snow firn. The snow density accuracy obtained by the use of this device is estimated to be near 12 % (Conger and McClung, 2009).

3.4 GPS

In December 2007, the initial observation network of 21 bamboo stakes was installed in a BIA on Union Glacier (Fig. 2). For each of these stakes GPS measurements were made using Topcon GR3 dual-frequency GPS receivers with measurement times of less than 30 s per stake, yielding metre-scale errors. In December 2008, 2009 and 2010, the same network as well as 35 new stakes were surveyed with dual-frequency Javad GPS model Lexon GGD receivers. In order to apply a differential correction procedure, a similar GPS receiver continuously collected data at a rock location (RX1 in Fig. 2). The precision obtained by these surveys improved to less than 10 cm by measuring between 15 and 30 min per stake. In addition, a dual-frequency Javad GPS receiver was installed on snow (Bstat in Fig. 2), collecting data between 11 December 2009 and 31 January 2010 for high-resolution studies (every 30 s), with the aim of detecting possible tidally modulated ice velocities. In January 2011, a real-time kinematic procedure was applied to data collected at the Union Glacier gate by a Leica SR 9500 receiver, with estimated decimetre accuracy. All GPS data collected were processed using the GrafNav 8.20 commercial software.

3.5 Surface elevation changes and geodetic mass balance estimation

The data obtained by the GPS measurements were compared in order to calculate the local mass balance and the absolute surface elevation changes in the BIA.

Using the measured height differences obtained by GPS and considering the surface topographic slope effect, the submergence/emergence velocity (w_e) was calculated:

$$w_e = w_s - u_s \tan\alpha, \quad (1)$$

where w_s is the vertical ice velocity, u_s is the ice velocity along the surface flow direction and α is the slope. The emergence velocity represents the vertical flow of ice relative to the glacier surface and allows the estimation of the net balance if it is assumed that density does not change with depth during the period (Hooke, 2005).

By subtracting the emergence velocity of the measured specific balance (stake height difference), the surface elevation change with time at a fixed position can be obtained.

$$\frac{\partial h}{\partial t} = b - w_e \quad (2)$$

If the glacier is in a steady state, there would be no surface changes, since accumulation and ablation compensate for the submergence and emergence velocities, so that the surface profile remains unchanged (Hooke, 2005). In this case $b = w_e$; however, most glaciers are not perfectly in steady state. Only the stake array measured at the Union gate was considered for this analysis.

3.6 Radar

A Coherent pulse compression radar depth sounder designed at Centro de Estudios Científicos CECs (Uribe et al., 2014) was used to measure ice thickness. The radar operates at a central frequency of 155 MHz, a maximum of 10 kHz of pulse repetition frequency (PRF), a bandwidth of 20 MHz and peak power of 200 W. Yagi antennae were used for both the transmitter and the receiver. We use two channels for simultaneous low and high signal amplification to increase the dynamic range of this radar.

A frequency-modulated continuous-wave (FM-CW) radar also designed by Uribe et al. (2014) was used to measure surface snow and ice layering to a depth of 450 m with a high vertical resolution (1 m). This radar works at a frequency from 550 to 900 MHz using two separated log periodic antennae for the transmitter and receiver. The transmit power was 21 dBm, and the whole system operated at a PRF of 10 kHz. A direct digital synthesis (DDS) system was used to generate an extremely linear frequency sweep transmitted signal.

The third radar system used along these tracks was a commercial ground-penetrating radar (GPR), a Geophysical Survey Systems Inc. (GSSI) model SIR-3000, working at 400 MHz. The range was set between 190 and 300 ns to record subsurface reflection with the aim of finding crevasses in real time. The GPR antennae were mounted on a 7 m long rod which was attached to a tractor and had a rubber car tyre tube installed at the opposite end. The radar data were analysed in real time while the tractor was moving, in order to

Table 2. Stake co-ordinates, velocities and mass balance per period. See Figs. 1 and 2 for locations.

Stakes	Lat.°	Lon.°	H. (m a e)	Velocity ($m\,a^{-1}$)	Mass balance (m w.eq. a^{-1})	Period	Type of surface
B1	−80.211	−81.230	803.12	12.7	0.18	2008–2009	Snow
B2	−80.124	−81.113	813.51	1.8	0.19		
B3	−80.045	−80.937	759.07	0.6	0.04		
B4	−79.985	−81.080	573.57	1.8	0.06		
B5	−79.922	−81.211	538.16	2.0	−0.07		Snow/BIA
B6	−79.840	−81.298	669.59	0.1	0.03		Snow
B7	−79.801	−81.348	553.87	1.2	0.04		
B8	−79.757	−81.965	459.99	2.9	0.14		
B9	−79.709	−82.455	531.04	33.3	0.14		
Bstat	−79.708	−82.454	531.34	33.0	–	2009/11/12 2010/31/01	
B10	−79.717	−82.643	639.79	34.6	0.17	2008–2009	
B11	−79.757	−82.803	672.46	20.5	0.13		
B12	−79.760	−82.931	690.56	20.9	0.20		
B13	−79.764	−83.091	703.53	22.9	−0.09		Ice
B14	−79.768	−83.266	738.39	22.4	−0.06		
B15	−79.798	−83.281	735.19	21.6	−0.16		
B16	−79.796	−83.316	742.20	23.2	−0.13		
B17	−79.765	−83.343	739.36	17.0	−0.08		Ice/crevasses
B18	−79.760	−83.370	747.68	14.0	−0.11		
B19	−79.764	−83.372	743.72	11.1	−0.10		
V00	−79.769	−83.370	739.47	18.1	−0.08	2008–2010	Ice
V01	−79.770	−83.370	738.44	19.0	−0.08	2007–2011	
V02	−79.772	−83.368	738.13	20.2	−0.04	2007–2010	
V03	−79.774	−83.365	739.69	21.7	−0.11	2007–2011	
V04	−79.775	−83.363	736.40	22.3	−0.07		
V05	−79.777	−83.361	733.57	23.0	−0.22		
V06	−79.779	−83.358	735.12	23.5	−0.11	2007–2010	
V07	−79.781	−83.355	736.61	23.9	−0.08		
V08	−79.784	−83.352	739.05	24.3	−0.13	2007–2009	
V09	−79.787	−83.343	738.60	24.3	−0.11	2007–2011	
V10	−79.790	−83.334	737.63	24.3	−0.13		
V11	−79.792	−83.325	738.82	24.0	−0.07	2007–2010	
V12	−79.771	−83.337	738.51	21.9	−0.09	2007–2011	
V13	−79.773	−83.335	735.87	22.3	−0.08		
V14	−79.774	−83.332	733.20	22.4	−0.08		
V15	−79.777	−83.327	731.27	22.7	−0.09		
V16	−79.779	−83.323	731.72	23.1	−0.10	2007–2009	
V17	−79.782	−83.316	731.16	23.4	−0.11	2007–2011	
V18	−79.784	−83.313	730.33	23.5	−0.13		
V19	−79.786	−83.309	729.48	23.6	−0.07		
V20	−79.788	−83.303	728.57	23.3	−0.11		
V21	−79.791	−83.298	733.66	23.0	−0.07		

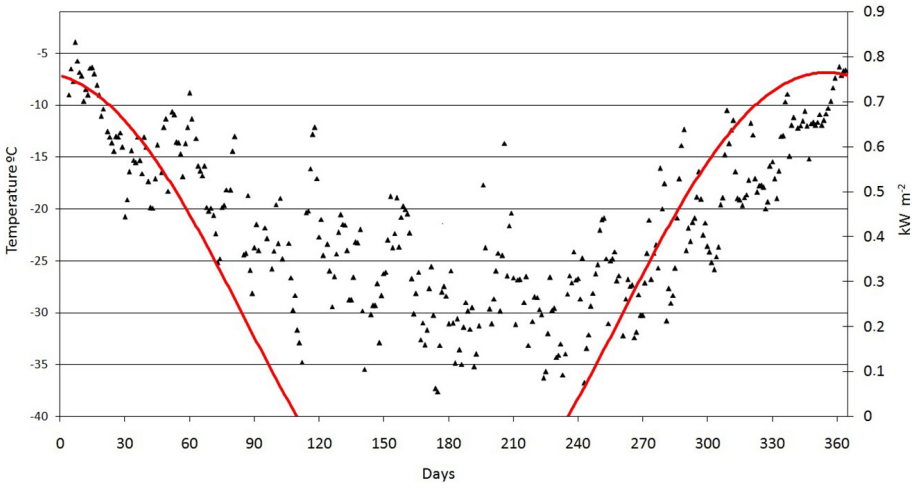

Figure 3. Mean daily temperature (°C) during 2008 (black triangles) and modelled solar direct radiation (red line) at the AWS site (kWm^{-2}).

alert the driver of the presence of hyperbolae potentially related to crevasses.

Post-processing and data analyses were carried out using Reflex-Win V5.6 (Sandmeier Scientific Software) for the three radar systems. Background removal, a dewow filter and adjustment of the gain function, among other procedures, were applied to the raw data. For crevasse analysis, migration correction procedures were also applied to collapse the hyperbolic diffractions to their proper point origins (Plewes and Hubbard, 2001). In order to convert travel time to ice thickness in metres, it was assumed that the electromagnetic wave travelled through the ice at $0.168\,m\,ns^{-1}$, a mean value representative of cold ice (Glen and Paren, 1975), and at $0.194\,m\,ns^{-1}$ assumed to be representative of snow/firn (Woodward and King, 2009).

4 Results

4.1 Meteorological data and BIA area changes

The meteorological data collected at Union Glacier between 2008 and 2013 contain several gaps and invalid records, but in general provide a good idea of the local conditions, which are especially useful for landing operations. In terms of climatological analysis, the series is too short and noisy, but is the only one available in the region.

The mean daily air temperature at this location (Fig. 3) from 2008 to 2012 was −20.6 °C, with an absolute minimum of −42.7 °C recorded on 12 August 2008 at 2 a.m. and an absolute maximum of 0.5 °C registered on 15 January 2010 at 8 p.m. Daily air temperatures have maximums in December–January following direct solar radiation; however, between April and August (included), when the Sun is below the horizon, the lowest temperatures have a mean of -25.5 ± 3.5 °C. Temperatures close to the melting point have only been observed in three summer events: 7–8 January 2008, 14–15 January 2010 and 25–26 December 2010, but no surface melting has been observed on this site. The mean air temperature in January is −10.3 °C.

Regarding wind speed and direction, the data are very consistent between 2008 and 2012, with a mean value of 16.3 knots and a predominant direction from 224°. The maximum wind speed recorded on site was near 60 knots and the predominant wind speeds are higher than 25 knots (Fig. 2). This predominant wind direction explains the extension of the main BIA, which experienced less than 10 % area change between 2002 and 2013. The available scene dates show some expected seasonal variability, especially when comparing more stable midsummer scenes (December–January) with early or late summer scenes (Brown and Scambos, 2005). The series is however too short to detect a trend (Table 1).

4.2 Surface mass balance

Snow densities measured at stakes drilled on snow surfaces have a mean value of $400 \pm 3\,kg\,m^{-3}$, with low variability between all surveyed stakes. No fresh and soft snow was detected due to the lack of precipitation in the region during our surveys. Table 2 indicates the details of each stake, the type of surface and the period of the measurements.

The surface mass balance estimations between 2007 and 2011 at the stakes installed on the BIA gate (V00 to V21, Table 2) are typically negative (Fig. 4), with a mean interannual surface mass balance of $-0.097\,m\,w.eq.\,a^{-1}$.

The stakes installed along the traverse between Patriot Hills and Union Glacier (Fig. 1) were only measured between 2008 and 2009 and showed differing results depending on their location. Stakes installed on snow surfaces (B1–B12) have positive mass balances, with a mean snow accumulation

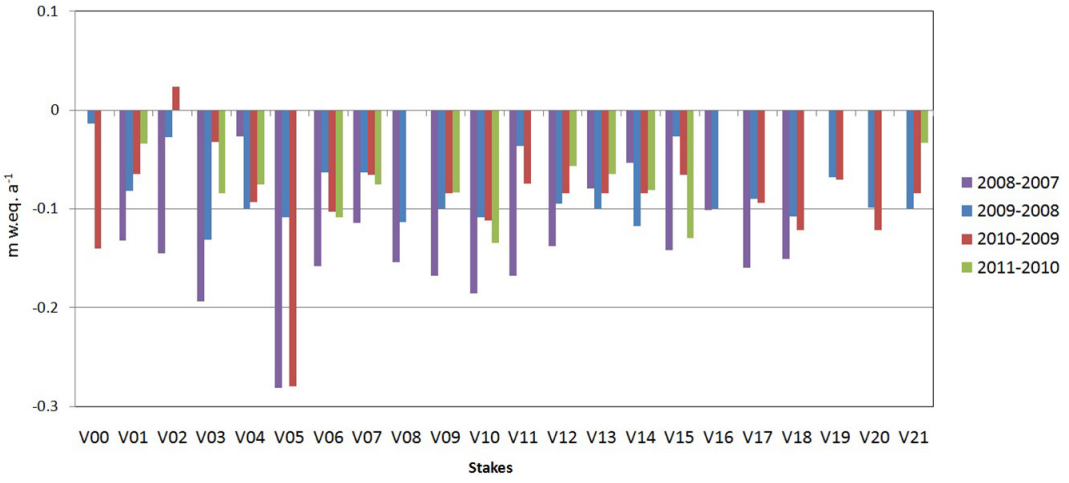

Figure 4. Mass balance (m w.eq. a^{-1}) for 2007–2011 at stakes located at the local BIA. Stake locations are shown in Fig. 2.

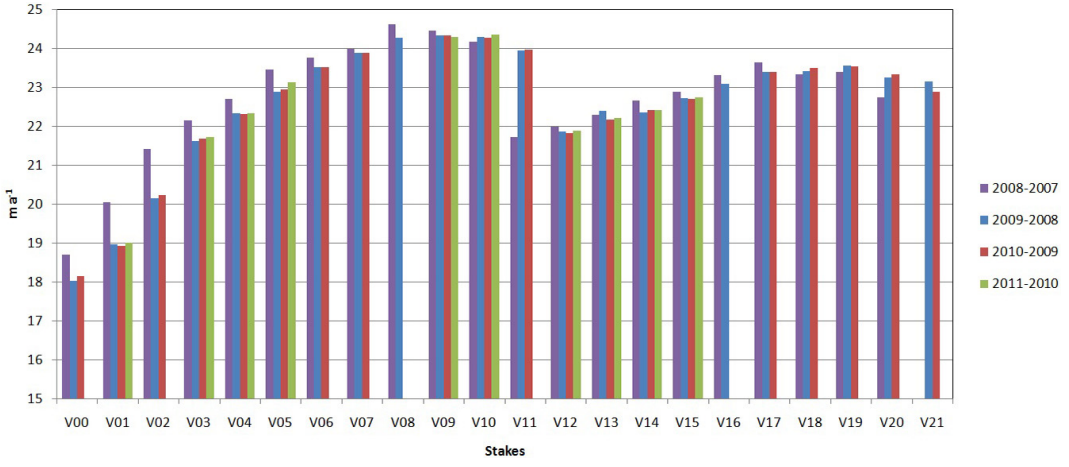

Figure 5. Ice velocities (m a^{-1}) at the Union Glacier gate by indicated years. Stake locations are shown in Fig. 2.

of 0.3 m a^{-1} (0.12 m w.eq. a^{-1}). Just outside the BIA, stake B12 showed the maximum net balance (0.2 m w.eq. a^{-1}), indicating that snow drift coming from the BIA due to the predominant katabatic wind direction (Fig. 2) is having a positive downstream accumulation effect. The only negative surface mass balance along the Patriot Hills–Union Glacier track (excluding the Union Glacier BIA) was detected at stake B5, which is located at the edge of the local BIA of the Plumber glacier (Fig. 1). Here a modest -0.07 m w.eq. a^{-1} (Table 2) was obtained between 2008 and 2009. Stakes B13–B19 (Table 2, Fig. 2) also had negative values, with a mean surface balance of 0.1 m w.eq. a^{-1}, coincident with the other stakes located at a local BIA.

4.3 Surface ice velocity

Surface ice velocities were obtained for 19 stakes (B1–B19) located along the track between Patriot Hills and the Union Glacier base camp (Figs. 1 and 2), with measurement periods of nearly 1 yr, and resulting ice velocities between 0.1 and 34.6 m a^{-1} (Table 2). Minimum values were observed at local ice divides (B2–B8), while the maximum velocity was observed at stake B10 located in the steepest area of Union Glacier, between two crevasse fields (Fig. 2).

Between 11 December 2009 and 31 January 2010, a dual-frequency GPS receiver was attached to stake Bstat, taking continuous measurements every 15 s. The receiver was powered by batteries and solar panels, providing a detailed record of daily ice dynamics during the spanned period of time. The main aim of this survey was to test the hypothesis that the ice dynamics of Union Glacier are affected by Ronne Ice Shelf tides, as has been observed at the Rutford Ice Stream, where a modulated ice flow was detected (Gudmundsson, 2006). This stake (Bstat, Table 2) is located 38 km upstream of the local grounding line zone of Constellation Inlet at the Ronne Ice Shelf (Figs. 1 and 2). The resulting ice velocity was 33 m a^{-1}, and thanks to the analysis carried out by

H. Gudmunsson (personal communication, 2010), no tidal effect was detected.

The neighbouring stake of Bstat (B9, located within a distance of 10 m) was only measured for 30 min in December 2009 and in December 2010, resulting in an annual velocity of $33.26 \pm 0.7\,\mathrm{m\,a^{-1}}$. The good correspondence with the Bstat results ($33\,\mathrm{m\,a^{-1}}$) indicates that Union Glacier does not show important seasonal ice velocity changes.

At the Union Glacier gate stake array (Fig. 2), 22 stakes were drilled into its blue ice area in 2007 and were resurveyed annually until 2011. Unfortunately, not all the original stakes have survived or were re-measured every year. However, from the remaining stake network a mean velocity of $20\,\mathrm{m\,a^{-1}}$ was estimated for the measurement period (Fig. 5). The overall ice motion at the gate is similar to the main wind direction (Fig. 2) observed in the BIA. No temporal velocity changes were observed during the studied period.

4.4 Surface elevation change

Considering the surface velocities obtained for the stakes (Table 2), and by applying Eq. (1), a mean vertical velocity for the blue ice of $-0.07 \pm 0.007\,\mathrm{m\,a^{-1}}$ was found at the Union Glacier gate. For a steady-state glacier this would be equal to the local mass balance; however, this is not the case for the studied area (there is a negative mass balance in the BIA), and a mean local elevation change of $-0.012\,\mathrm{m\,a^{-1}}$ was found. In any case, this result is close to the estimated error of the measurements and indicates near-equilibrium conditions.

4.5 Glacier thickness and internal structure

More than 450 km of radar tracks were measured between 2008 and 2010 in the Union Glacier area, including oversnow traverses between Patriot Hills, Union Glacier and the high Antarctic plateau.

The 80 km long profile between the Antarctic plateau and Union Glacier (Fig. 6 upper), including the transit along the Balish, Schneider, Schanz and Driscoll glaciers, was surveyed with a FM-CW radar for snow accumulation data, a compression pulse radar for ice thickness data and a GPR system for crevasse detection purposes.

The deep ice of the plateau is seen at the beginning of the survey profile (A in Fig. 6), and is then followed by a passage characterised by shallow ice (B) where the steepest section of the whole traverse was crossed. After this section, the thickness increases sharply until a local maximum thickness of 1120 m was observed at Balish Glacier. The local divide between the Balish and Schneider glaciers (C in Fig. 6) has a prominent subglacial peak (C in Fig. 6) where the mountain range dividing the two glaciers is also visible underneath the ice. The maximum thickness measured at Schneider Glacier was 900 m, 1050 m at Schanz Glacier, 1510 m at Driscoll Glacier and 1540 m at Union Glacier, close to the base camp. The mean ice thickness measured at Union Glacier was 1450 m. The subglacial topography in the valley is smooth, with "U"-shaped flanks.

At the beginning of the radar profile (A–B in Fig. 6), it is possible to see the shallowest ice at the Gifford Peaks pass (passage), with a thickness between 45 and 140 m obtained by the low-gain channel of the pulse compression radar. This profile is not visible in the high-gain channel, due to set-up constraints on this system (Uribe et al., 2014).

The FM-CW radar detected multiple internal snow–firn layers and the snow–ice boundary layer with a high resolution. Figure 7 shows an FM-CW profile at Union Glacier, where the snow–ice boundary layer is at a depth of 30–40 m (between A and B in Fig. 7) and then tends to disappear when approaching the BIA (between C and D in Fig. 7). The central moraine line of the glacier is indicated by the letter C in Fig. 7.

The GPR data collected along the track from Union Glacier to the Antarctic plateau allowed the detection of many crevasses both near the runway area and at the Gifford Peaks passage, just before reaching the plateau. Along the survey route the GPR system was able to detect the upper 20 m of the internal structure of the ice. Within this upper layer, annual snow/firn layers suffered (in places) discontinuities due to crevasses that appeared as hyperbolae on the radar traces.

In general, the route from Union Glacier to the Antarctic plateau is almost totally free of crevasses. An exception to this was the Gifford passage (B in Fig. 6), where a minor system of crevasses was detected, with widths between 1 and 5 m and snow bridges between 1.5 and 3 m thick. In spite of these crevasses, the Gifford passage is the shortest (235 km) gateway for oversnow traverses from Union Glacier to the Subglacial Lake Ellsworth (Vaughan et al., 2007) on the Antarctic plateau. The alternative route to this subglacial lake is nearly 520 km long, starting at Union Glacier, passing along Patriot Hills, then travelling around the Three Sails and finally turning west toward the Subglacial Lake Ellsworth (Fig. 1).

5 Discussion

At Union Glacier, the local BIA is shaped by strong snowdrift caused by katabatic winds accelerated by the slope at the main junction between the two glacial valley arms feeding Union Glacier from the upper Antarctic plateau. As a result, the net mass balance at this BIA is negative, the driving factor explaining the mass losses being sublimation of ice during summer months, as no melting event has been observed since 2007. However, melting events have been observed in the region, especially at Patriot Hills, where a small water pond was formed at the boundary between the BIA and the nunatak during a very warm 1997 summer (Carrasco et al., 2000).

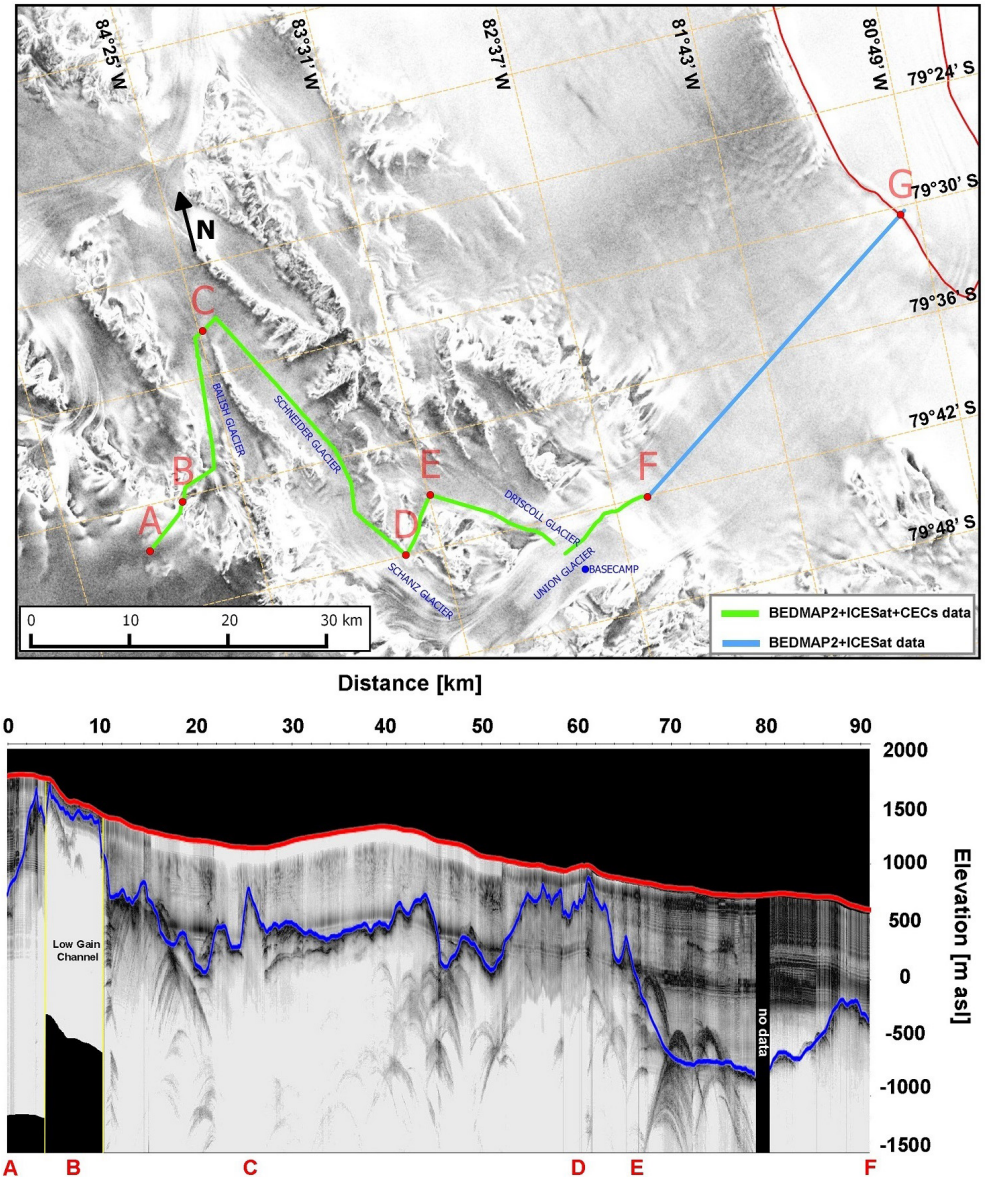

Figure 6. Top: location map of the radar and GPS survey measured between the Antarctic Plateau (A) and Union Glacier (F) in 2010 (green line). In blue, the available data between F and the local grounding line zone (in red, from Rignot et al., 2011a) at Constellation Inlet (G). The background image is the RAMP AMM-1 SAR Image Mosaic of Antarctica (Jezek and RAMP Product Team, 2002). Bottom: surface (red line) and subglacial topography (blue line) interpreted from the radar data collected in 2010 along the A–F track.

In spite of this negative surface mass balance, the resulting ice elevation changes between 2008 and 2011 at the Union gate are very close to the error of the measurements (combined error of 0.01 m), with a mean of $-0.012\,\mathrm{m\,a^{-1}}$ and high spatial variability ($\pm 0.044\,\mathrm{m\,a^{-1}}$) among the gate stakes. Accordingly, the glacier must be considered in equilibrium, without significant changes compared with previous data (Rivera et al., 2010).

The ice velocities at the BIA fluctuate between 11 and $24\,\mathrm{m\,a^{-1}}$, without significant changes between 2007 and 2011. However, downstream of the Union gate, the velocities increase up to $33\,\mathrm{m\,a^{-1}}$ at the continuous GPS stake (Bstat), where no seasonal variations or tidally modulated variability were detected.

The GPR survey allowed the detection of many more crevasses than were previously mapped with the ASTER imagery (Rivera et al., 2014). The 400 MHz GPR is capable of identifying in real time surface and buried crevasses. The crevasse data were compared with the FM-CW records and in most of the cases the wider crevasses (2 to 4 m width) could be detected in both radars. However, the FM-CW radar did not provide the best information in regards to snow bridge

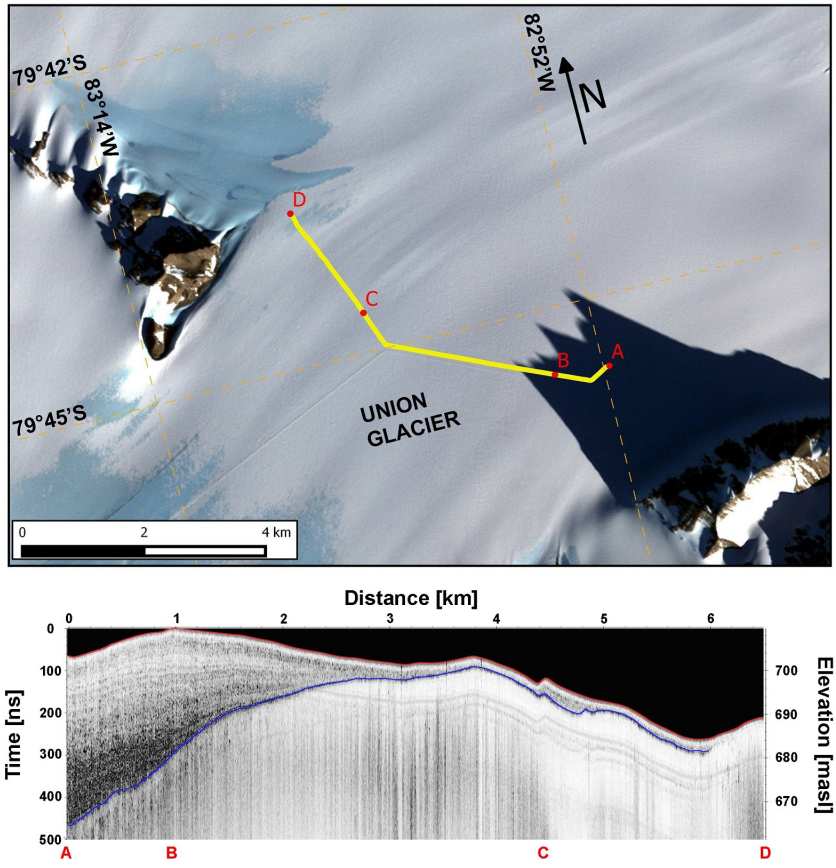

Figure 7. FM-CW data obtained at Union Glacier. Top: location of the surveyed track near the base camp of Union Glacier. The background image is an ASTER false composite 321 acquired on 14 March 2013. Bottom: radargram showing the surface topography (red line), internal annual snow/firn layers and the firn/ice boundary (blue line). Letters A and B indicate the base camp where the snow/firn layers are near 30–40 m thickness in total. Letter C corresponds to the medial moraine line of the glacier. Letter D indicates the appearance of the BIA at the surface.

thicknesses (less than 1 m), its resolution being insufficient to detect the first metres of the snow pack.

Comparisons of surface and bedrock topography along transect A–F (Fig. 8) resulted in a maximum ice thickness difference of 1447 m, with a mean difference of 477 m (standard deviation 348 m) between the data presented here and BEDMAP2 (Fretwell et al., 2013). The surface topography of the surveyed traverse was found to differ from BEDMAP2 and ICESat (2003–2005) by means of 91 and 169 m, respectively. These differences are understandable due to the coarse resolution of BEDMAP2 and the footprint of ICESat.

The subglacial topography (Fig. 8) at the main trunk of Union Glacier toward the local GLZ (Segment E–G in Fig. 6) showed a subglacial topography well below sea level (near −858 m), much deeper than previously estimated by BEDMAP2. However, between Union Glacier and the local GLZ, the subglacial topography shows a maximum altitude of −190 m at F in Figs. 6 and 8. The subglacial topography then deepens toward the GLZ, where the bedrock is estimated to be 1050 m below sea level (Fretwell et al., 2013). This subglacial condition implies that an upstream migration of the GLZ until point F in Figs. 6 and 8 will not have a strong effect on Union Glacier. However, the glacier can respond in a more dynamic way if this possible migration affects Union Glacier upstream of this potential pinning point.

6 Conclusions

Several glaciological oversnow campaigns have been undertaken to Union Glacier and nearby areas since 2007, where the surface and subglacial topographies were mapped in detail. These results were compared with the BEDMAP2 data set, showing much deeper bedrock and a much more complex subglacial topography. The obtained results determined a maximum ice thickness of 1540 m in Union Glacier, with a maximum snow ice boundary layer at 120 m. The internal structure of the ice was also mapped, including the detection of isochronous layers and crevasses, allowing logistic operators and scientists to work along safer routes.

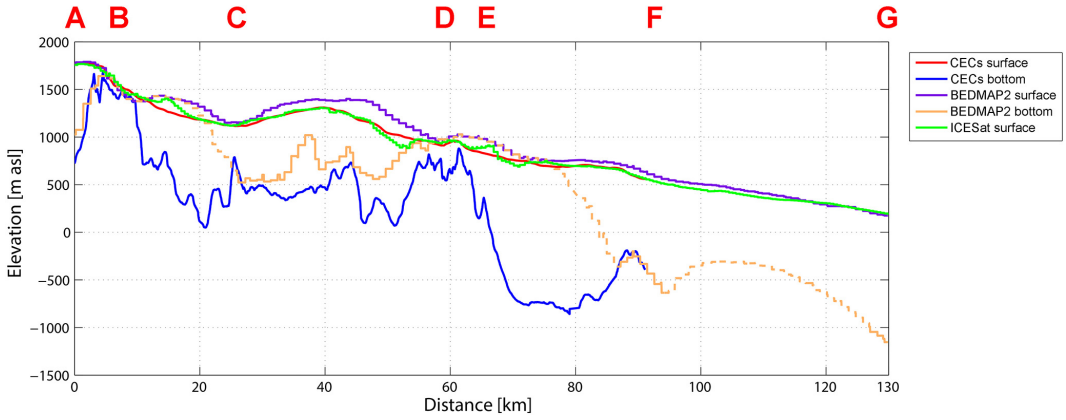

Figure 8. Comparisons of surface and bedrock topography of different data sources along transect A–G (see the upper panel of Fig. 6 for the location of the transect). CEC surface and bedrock from the year 2010. ICESat surface from 2003 to 2005, BEDMAP2 surface and bedrock from Fretwell et al. (2013). The BEDMAP2 bottom dashed line is interpolated.

Ice dynamics were also recorded thanks to the measurement of ice velocities and ice thicknesses. Maximum ice velocity values of 34.6 m a^{-1} were obtained. Near-equilibrium conditions were calculated at the BIA, where mean velocities of 20 m a^{-1} were measured. The snow accumulation among the studied stakes outside the BIA showed values of up to 0.2 m w.eq. a^{-1} (near 0.5 m a^{-1} of snow). At the BIA, a local negative mass balance was detected as expected, with mean ablation rates of 0.1 m w.eq. a^{-1}.

Due to the below sea level subglacial topography upstream of the local GLZ, it is expected that Union Glacier can experience some thinning and acceleration in future scenarios of GLZ migration. However, these impacts will not affect the whole glacier, because at near 55 km upstream of the present GLZ, the bedrock topography has a prominent ridge perpendicular to the main ice flow direction, where the bedrock has a maximum altitude of −190 m a.s.l. This ridge can play an important role in modulating future glacier responses by enabling the grounding line to come to a prolonged standstill, providing the glacier with a "pinning point".

Overall, the collected data allowed a ground route from Union Glacier to the upper Antarctic plateau to be mapped satisfactorily. The route is important, as it traverses the Subglacial Lake Ellsworth and the main ice streams flowing into the Amundsen Sea Embayment area (Pine Island Glacier) and toward the Weddell Sea (Institute and Rutford ice streams). This new 235 km long route toward the Subglacial Lake Ellsworth is shorter than half of the previously traversed track of 517 km, providing a much more direct and shorter gateway to inner Antarctica.

Acknowledgements. This research was supported by Antarctic Logistic Expeditions (ALE) Ltd. Special thanks to M. Sharp, P. McDowell, C. Jacobs, Eddy, Boris and all ALE personnel at Union Glacier. CECs is funded by the Basal fund of CONICYT, among other grants. J. A. Neto collaborated with GPS data collection in 2011. A. Wendt, C. Rada, T. Kohoutek and M. Barandun helped with data processing. H. Gudmundsson analysed the GPS data at Bstat in order to detect possible tidally modulated effects on the ice flow. J. Carrasco and F. Burger helped with the met data. D. Carrión helped with figures and satellite image analysis. R. Wilson edited the text. The GLIMS project provided ASTER data. A. Rivera is a Guggenheim fellow. The comments and suggestions by Ted Scambos and Neil Ross are highly appreciated.

Edited by: E. Larour

References

Bamber, J., Riva, R., Vermeersen, B., and LeBrocq, A.: Reassessment of the potential. Sea-level rise from a collapse of the West Antarctic Ice Sheet Science, Science, 324, 901–903, 2009.

Brown, I. and Scambos, T.: Satellite monitoring of blue ice extent near Byrd Glacier, Antarctica, Ann. Glaciol., 39, 223–230, 2005.

Carrasco, J., Casassa, G., and Rivera, A.: A warm event at Patriot Hills, Antarctica: An ENSO related phenomena?, in: Sixth International Conference on Southern Hemisphere Meteorology and Oceanography, 240–241, Santiago, Chile, 2000.

Cavalieri, D. and Parkinson, C.: Antarctic sea ice variability and trends, 1979–2006, J. Geophys. Res., 113, C07004, doi:10.1029/2007JC004564, 2008.

Conger, S. and McClung, D.: Comparison of density cutters for snow profile observations, J. Glaciol., 55, 163–169, 2009.

Fretwell, P., Pritchard, H., Vaughan, D., Bamber, J., Barrand, N., Bell, R., Bianchi, C., Bingham, R., Blankenship, D., Casassa, G., Catania, G., Callens, D., Conway, H., Cook, A., Corr, H., Damaske, D., Damm, V., Ferraccioli, F., Forsberg, R., Fujita, S., Gim, Y., Gogineni, P., Griggs, J., Hindmarsh, R., Holmlund, P., Holt, J., Jacobel, R., Jenkins, A., Jokat, W., Jordan, T., King, E., Kohler, J., Krabill, W., Riger-Kusk, M., Langley, K., Leitchenkov, G., Leuschen, C., Luyendyk, B., Matsuoka, K., Mouginot, J., Nitsche, F., Nogi, Y., Nost, O., Popov, S., Rignot, E., Rippin, D., Rivera, A., Roberts, J., Ross, N., Siegert, M., Smith, A., Steinhage, D., Studinger, M., Sun, B., Tinto, B.,

Welch, B., Wilson, D., Young, D., Xiangbin, C., and Zirizzotti, A.: Bedmap2: improved ice bed, surface and thickness datasets for Antarctica, The Cryosphere, 7, 375–393, doi:10.5194/tc-7-375-2013, 2013.

Glen, J. and Paren, J.: The electrical properties of snow and ice, J. Glaciol., 15, 15–38, 1975.

Gudmundsson, G.: Fortnightly variations in the flow velocity of Rutford Ice Stream, West Antarctica, Nature, 444, 1063–1064, 2006.

Hellmer, H., Kauker, F., Timmermann, R., Determann, J., and Rae, J.: Twenty "first" century warming of a large Antarctic ice-shelf cavity by a redirected coastal current, Nature, 485, 225–228, 2012.

Hooke, R.: Principles of Glacier Mechanics, Cambridge University Press, Cambdridge, UK, 2nd edn., 2005.

Jezek, K. and RAMP Product Team: RAMP AMM-1 SAR Image Mosaic of Antarctica. Version 2. Fairbanks, AK: Alaska Satellite Facility, in association with the National Snow and Ice Data Center, Boulder, CO. Digital media, 2002.

Joughin, I. and Bamber, J.: Thickening of the ice stream catchments feeding the Filchner-Ronne Ice Shelf, Antarctica, Geophys. Res. Lett., 32, L17503, doi:10.1029/2005GL023844, 2005.

Mayewski, P., Meredith, M., Summerhayes, C., Turner, J., Worby, A., Barrett, P., Casassa, G., Bertler, N., Bracegirdle, T., Naveira, A., Bromwich, D., Campbell, H., Hamilton, G., Lyons, W., Maasch, K., Aoki, S., Xiao, C., and van Ommen, T.: State of the Antarctic and Southern Ocean climate system, Review of Geophysics, 47, RG1003, doi:10.1029/2007RG000231, 2009.

Paterson, W.: The physics of glaciers, Pergamon Press, Great Britain, 3rd edn., 1994.

Plewes, A. and Hubbard, B.: A review of the use of radio-echo sounding in glaciology, Prog. Phys. Geog., 25, 203–236, 2001.

Rignot, E. and Jacobs, S.: Rapid bottom melting widespread near Antarctic Ice Sheet grounding lines, Science, 296, 2020–2023, 2002.

Rignot, E. and Thomas, R.: Mass balance of polar ice sheets, Science, 297, 1502–1506, 2002.

Rignot, E., Vaughan, D., Schmeltz, M., Dupont, T., and MacAyeal, D.: Acceleration of Pine Island and Thwaites Glaciers, West Antarctica, Ann. Glaciol., 34, 189–194, 2002.

Rignot, E., Mouginot, J., and Scheuchl, B.: Antarctic grounding line mapping from differential satellite radar interferometry, Geophys. Res. Lett., 38, L10504, doi:10.1029/2011GL047109, 2011a.

Rignot, E., Mouginot, J., and Scheuchl, B.: Ice Flow of the Antarctic Ice Sheet, Science, 333, 1427–1430, 2011b.

Rivera, A., Zamora, R., Rada, C., Walton, J., and Proctor, S.: Glaciological investigations on Union Glacier, Ellsworth Mountains, West Antarctica, Ann. Glaciol., 51, 91–96, 2010.

Rivera, A., Cawkwell, F., Wendt, A., and Zamora, R.: Mapping Blue Ice Areas and Crevasses in West Antarctica Using ASTER Images, GPS and Radar Measurements, in: Global Land Ice Measurements from Space, edited by: Kargel, J., Leonard, G., Bishop, M., Kääb, A., and Raup, B., chap. 31, 743–757, Springer-Praxis, Heidelberg, 2014.

Ross, N., Bingham, Corr, H., Ferraccioli, F., Jordan, T., Le Brocq, A., Rippin, D., Young, D., Blankenship, D., and Siegert, J.: Steep reverse bed slope at the grounding line of the Weddell Sea sector in West Antarctica, Nat. Geosci., 5, 393–396, 2012.

Scambos, T., Haran, T., Fahnestock, M., Painter, T., and Bohlander, J.: MODIS-based Mosaic of Antarctica (MOA) data sets: continent-wide surface morphology and snow grain size, Remote Sens. Environ., 111, 242–257, 2007.

Uribe, J., Zamora, R., Gacitúa, G., Rivera, A., and Ulloa, D.: A low power consumption radar system for measuring ice thickness and snow/firn accumulation in Antarctica, Ann. Glaciol., 55, 39–48, 2014.

Vaughan, D., Rivera, A., Woodward, J., Corr, H., Wendt, J., and Zamora, R.: Topographic and hydrological controls on Subglacial Lake Ellsworth, West Antarctica, Geophys. Res. Lett., 34, L18501, doi:10.1029/2007GL030769, 2007.

Wendt, A., Casassa, G., Rivera, A., and Wendt, J.: Reassessment of ice mass balance at Horseshoe Valley, Antarctica, Antarct. Sci., 21, 505–513, 2009.

Woodward, J. and King, E.: Radar surveys of the Rutford Ice Stream onset zone, West Antarctica: indications of flow (in)stability?, Ann. Glaciol., 50, 57–62, 2009.